Gene 518 (2013) 52–58

Contents lists available at SciVerse ScienceDirect

Gene

journal homepage: www.elsevier.com/locate/gene

Deriving correlated motions in proteins from X-ray structure refinement by using TLS parameters

Yen-Yi Liu, Chien-Hua Shih, Jenn-Kang Hwang, Chih-Chieh Chen *

Institute of Bioinformatics and Systems Biology, National Chiao Tung University, Hsinchu 30068, Taiwan, ROC

ARTICLE INFO

Available online 24 December 2012

Keywords:
TLS parameter
TLS model
Correlated motion
Atomic cross-correlation

ABSTRACT

Dynamic information in proteins may provide valuable information for understanding allosteric regulation of protein complexes or long-range effects of the mutations on enzyme activity. Experimental data such as X-ray B-factors or NMR order parameters provide a convenient estimate of atomic fluctuations (or atomic auto-correlated motions) in proteins. However, it is not as straightforward to obtain atomic cross-correlated motions in proteins — one usually resorts to more sophisticated computational methods such as Molecular Dynamics, normal mode analysis or atomic network models. In this report, we show that atomic cross-correlations can be reliably obtained *directly* from protein structure using X-ray refinement data. We have derived an analytic form of atomic correlated motions in terms of the original TLS parameters used to refine the B-factors of X-ray structures. The correlated maps computed using this equation are well correlated with those of the method based on a mechanical model (the correlation coefficient is 0.75) for a non-homologous dataset comprising 100 structures. We have developed an approach to compute atomic cross-correlations *directly* from X-ray protein structure. Being in analytic form, it is fast and provides a feasible way to compute correlated motions in proteins in a high throughput way. In addition, avoiding sophisticated computational operations; it provides a quick, reliable way, especially for non-computational biologists, to obtain dynamics information directly from protein structure relevant to its function.

1. Introduction

Protein dynamics is important for protein functions (Kubitzki et al., 2009; Rasmussen et al., 1992). Studies for several well-known proteins, such as myoglobin (Austin et al., 1975; Elber and Karplus, 1987; Parak and Knapp, 1984), hemoglobin (Ansari et al., 1986; Case and Karplus, 1979) and lysozyme (Karplus and Post, 1996; Post et al., 1986; Strynadka and James, 1996), indicate the significance of dynamics relation to functions. The B-factor, acquired from an X-ray crystal structure, represents the fluctuation of an atom about its mean position. There have been many reports of applying the B-factor to investigations into protein functions (Altman et al., 1994; Carugo and Argos, 1998; Parthasarathy and Murthy, 2000; Radivojac et al., 2004; Yuan et al., 2003). In addition to atomic fluctuations in position, correlations between the fluctuations of residues in proteins are important to understanding the mechanisms of protein function. Examples include the gating mechanism of mechanosensitive channel (Valadie et al., 2003), the anesthetic inhibition mechanism of the firefly luciferase (Szarecka et al., 2007a), the anesthetics targeting of neuronal α4β2 nicotinic acetylcholine receptor (Szarecka et al., 2007b), the hinge regions of human copper transporter 1 (Schushan et al., 2010), the catalysis of α-chymotrypsin (Solá and Griebenow, 2006) and the allosteric signaling in catabolite activator protein (Toncrova and McLeish, 2010). However, correlations between the displacements of atoms cannot be determined from the X-ray experimental data (Winn et al., 2001). The Molecular Dynamics computational method (Brooks et al., 1988; Levitt and Warshel, 1975; McCammon and Harvey, 1986; McCammon et al., 1977; Rueda et al., 2007; Warshel, 1976, 2002) and normal mode analysis (Brooks and Karplus, 1983; Kidera and Go, 1992; Levitt et al., 1985) are the most common ways used to determine the correlated fluctuations between residues. These approaches model protein structures that apply a mechanical force field (Brooks et al., 1983; Jorgensen and Tirado-Rives, 1988; Ponder and Case, 2003; Scott et al., 1999) to compute protein motions using long-time trajectory integration or matrix diagonalization.

TLS refinement (Winn et al., 2001) is a B-factor refinement method integrated in the REFMAC software program (Murshudov et al., 1997). Optimization of the TLS (Translation/Libration/Screw) parameters is the key to this method, because these are used for describing the molecular motions in crystals, based on X-ray data (Cruickshank, 1956; Schomaker and Trueblood, 1968). The TLS parameters have

Abbreviations: TLS, Translation/Libration/Screw; GNM, Gaussian network model; NADH, nicotinamide-adenine dinucleotide (reduced form); NADPH, nicotinamide-adenine dinucleotide phosphate; PDB, Protein Data Bank.

* Corresponding author at: 75 Bo-Ai Street, Hsinchu, 30068, Taiwan, Republic of China. Tel.: +886 3 5729287; fax: +886 3 5729288.

E-mail addresses: yyl.bi97g@nctu.edu.tw (Y.-Y. Liu), scwnctu.bi94g@nctu.edu.tw (C.-H. Shih), jkhwang@cc.nctu.edu.tw (J.-K. Hwang), chieh.bi91g@nctu.edu.tw (C.-C. Chen).

0378-1119/$ – see front matter © 2012 Elsevier B.V. All rights reserved.
http://dx.doi.org/10.1016/j.gene.2012.11.086

been successfully used for modeling atomic displacements from experimental X-ray data (Sternberg et al., 1979). Here, we show that correlated motions can be determined directly from refined X-ray structures by using TLS parameters, without the need for additional simulations.

Because of the difficulty of obtaining atomic cross-correlations experimentally, we evaluate our method using correlation maps computation based on the Gaussian network model (GNM) (Bahar et al., 1997; Ming et al., 2002; Tirion, 1996) — a coarse-grained version of the normal model analysis approach, as a reference standard. In this paper, we compare correlation maps calculated using our method and those produced using normal mode methodologies, and discuss several applications of our method in the context of protein function.

2. Methods

2.1. The empirical model for computing the atomic cross-correlation by using TLS parameters

Based on the TLS model (Schomaker and Trueblood, 1968), we represent the correlation between isotropic displacements of an atom as a function of the spatial coordinated and the TLS parameters, defined by Sternberg et al. (Sternberg et al., 1979) as:

$$\langle \Delta \mathbf{r}_i \cdot \Delta \mathbf{r}_i \rangle = \frac{1}{3}\mathbf{tr}\left(\mathbf{T} + \mathbf{S}^{\mathbf{T}} \times \mathbf{n} - \mathbf{n} \times \mathbf{S} - \mathbf{n} \times \mathbf{L} \times \mathbf{n}\right), \quad (1)$$

Where, $\Delta \mathbf{r}_i$ refers to the isotropic displacements of an atom; $\mathbf{T} \equiv \mathbf{t}\mathbf{t}^{\mathbf{T}}$, $\mathbf{L} \equiv \lambda\lambda^{\mathbf{T}}$ and $\mathbf{S} \equiv \lambda\mathbf{t}$ represent the translation, libration and screw matrixes, respectively. We will refer to the atomic cross-correlation computed based on Eq. (1) as B_{TLS}. The translation matrix **T** is constructed from the displacement correlations between translation vectors along three directions $\mathbf{t}_x$, $\mathbf{t}_y$ and $\mathbf{t}_z$. The libration matrix **L** contains the displacement correlations between rotation vectors about three axes λ_x, λ_y and λ_z. Correlations between the translation and rotation vectors are used to build the screw matrix **S**. Each of **T**, **L**, and **S** is a 3×3 matrix, where **T** and **L** are symmetric matrixes, and **S** is usually with arbitrarily specified origin. Position relative to the origin of an atom is specified by **n**. In total, 10 TLS parameters are refined to obtain the required atomic fluctuation (Sternberg et al., 1979).

Based on the atomic fluctuation equation derived from the TLS parameters, it is not hard to present the cross-correlation between isotropic displacements of atom *i* and atom *j* in the same TLS group as:

$$\left\langle \Delta \mathbf{r}_i \cdot \Delta \mathbf{r}_j \right\rangle = \frac{1}{3}\mathbf{tr}\left(\mathbf{T} + \mathbf{S}^{\mathbf{T}} \times \mathbf{n}_j^{\mathbf{T}} - \mathbf{n}_i \times \mathbf{S} - \mathbf{n}_i \times \mathbf{L} \times \mathbf{n}_j^{\mathbf{T}}\right). \quad (2)$$

Where, $\mathbf{n}_i$ and $\mathbf{n}_j$ are the positions of atom *i* and atom *j* with regard to an arbitrary origin O, respectively. We will refer to the atomic cross-correlation computed based on Eq. (2) as CC_{TLS}. Additionally, we should note that the TLS parameters used in Eq. (2) are identical to those in Eq. (1), and if $i = j$ the CC_{TLS} is equivalent to B_{TLS}, which is the same as the value given by Eq. (1). This means that we can use the TLS parameters obtained from TLS refinement directly to compute both CC_{TLS} and B_{TLS} by applying Eq. (2).

2.2. The TLS parameter refinement

TLS parameters are commonly optimized in one of the two ways: by direct comparison with X-ray diffraction data (Driessen et al., 1989; Howlin et al., 1993; Winn et al., 2001) and by fitting to an existing set of refined temperature factors (He and Craven, 1993; Kuriyan and Weis 1991; Sternberg et al., 1979). An entire protein molecule is treated as a rigid body or as the combination of several rigid fragments (i.e., several TLS group). Although a protein structure can frequently be subdivided into multiple TLS groups, in this study we only consider the situation that each chain of a given protein structure is treated as a TLS group. Later, we discuss the effect of treating each domain in a protein as a separate TLS group. In refining TLS parameters based on X-ray crystallography data, the protein coordinates and X-ray experimental data are used as the initial input data for REFMAC software program. In general, 10–15 cycles of the TLS refinement are followed by 10 cycles of maximum likelihood restrained refinement. The obtained TLS parameters can be used for computing dynamic cross-correlations after the R/R_{free} ratio becomes a stable function of the refinement cycles, and of the TLS group parameters converge. Because the coordinates change as refinement processes (resulting from restrained refinement), the final optimized coordinates obtained from the TLS refinement are used as the input data for computing the dynamic correlations in the X-ray spectral PDB file.

2.3. Similarity between correlation maps

For easy analysis, atomic correlations are usually presented as correlation maps with the auto- and the cross-correlations at the diagonal and the off-diagonal entries of the matrix, respectively. To compare the correlation maps computed using our method (**C**) and the GNM (**G**), we used Pearson's correlation coefficient to measure the similarity:

$$r = \frac{\sum_a \sum_b \left(c^{ab} - \bar{c}\right)\left(g^{ab} - \bar{g}\right)}{\sqrt{\left(\sum_a \sum_b \left(c^{ab} - \bar{c}\right)\right)^2 \left(\sum_a \sum_b \left(g^{ab} - \bar{g}\right)\right)^2}}. \quad (3)$$

Where, c^{ab} and g^{ab} are elements in correlation maps **C** and **G**; $\bar{c}$ and $\bar{g}$ are the element's mean values.

2.4. Dataset

To evaluate our method, we choose 100 non-redundant X-ray proteins with sequence identity ≤25% from PISCES (Wang et al., 2003). The protein sizes for this set are between 100 and 600 residues in a single chain, at a resolution ≤2 Å. TLS refinement has been carried out on all of the selected structures, assigning a single TLS group per chain using the REFMAC software program. The dataset chains are listed in Table S1 in the supplementary material. Hereinafter, we refer to this dataset as "100-dataset".

3. Results

3.1. Comparison of correlation maps and the slowest normal modes computed using our method and the GNM

For convenience, atomic displacement correlations are usually presented as correlation maps. Here, we compared several maps calculated using our method with those determined using the GNM. Comparisons of correlation maps calculated using our method and the GNM for N-terminal actin depolymerizing factor homology domain of Human twinfilin-2 (PDB ID: 2VAC:A), bovine neurexin 1 alpha LNS/LG domain 4 (PDB ID: 2R16:A), aminomethyltransferase of glycine cleavage system (PDB ID: 1VLO:A) and tyrosine phosphatase 1B (PDB ID: 2F71:A) are shown in Fig. 1. Each of these four pairs of maps is in excellent agreement. The normal mode vectors and frequencies can be calculated by diagonalizing the Hessian matrix. Because the inverse correlation matrix is the Hessian matrix, we obtain the normal mode vectors by simply inverting and diagonalizing the correlation matrix. Many studies report that the lowest-frequency motions of the normal modes often relate to protein functions (Amadei et al., 1993; Brooks and Karplus, 1983; Hinsen, 1998, 2000; Tama and Sanejouand, 2001; Thomas et al., 1999). Fig. 2 shows that the comparisons between the slowest normal modes calculated by our method and

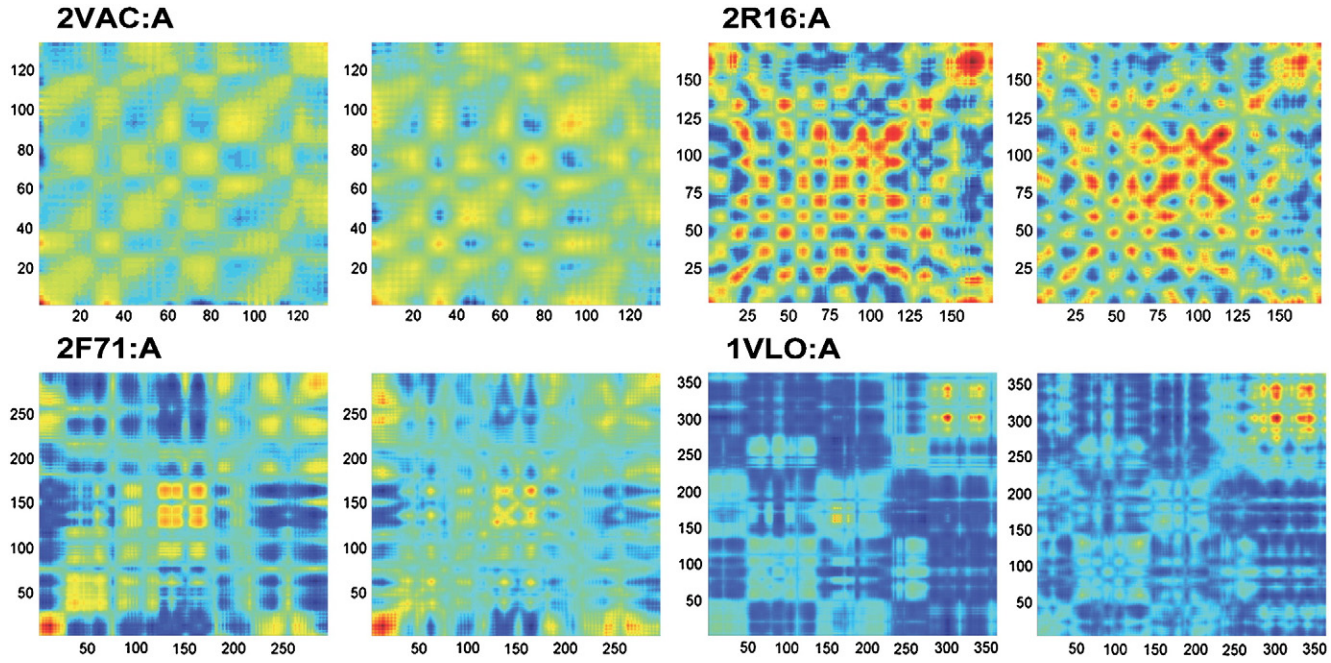

Fig. 1. Correlation maps for some of the proteins from the 100-dataset. For each protein case, the left panel is the map computed by our method and the right by the GNM. The colors of the map ramp from red (positive correlation) to blue (negative correlation).

the GNM for those structures examined in Fig. 1 are in excellent agreement.

3.2. Large-scale evaluation of our method

For large-scale evaluation, we used Eq. (3) to measure the similarity between the correlation maps. Fig. 3 shows the distribution of correlation coefficients between pairs of the correlation maps produced by our method and the GNM for the 100-dataset. The average correlation coefficient is $\bar{c} = 0.75$ and the fraction of structures with the correlation coefficient larger than 0.75 is 0.58.

3.3. The breakdown analysis for the accuracy of our method

We tested seven protein characteristics to determine the accuracy of our method in computing atomic cross-correlations. Of these characteristics, protein size, mean B-factor and function are related to protein properties, while solvent contents and crystal lattices are used to describe the environmental condition of a crystalline protein molecule. The remaining two characteristics, the R-value, and X-ray structure resolution are applied to represent the quality of a crystal structure. Figs. 4A–C present performance profiles for our method as a function of protein size, mean B-factor, and the top 5 quantity protein functions (hydrolase, transferase, oxidoreductase, lyase, and

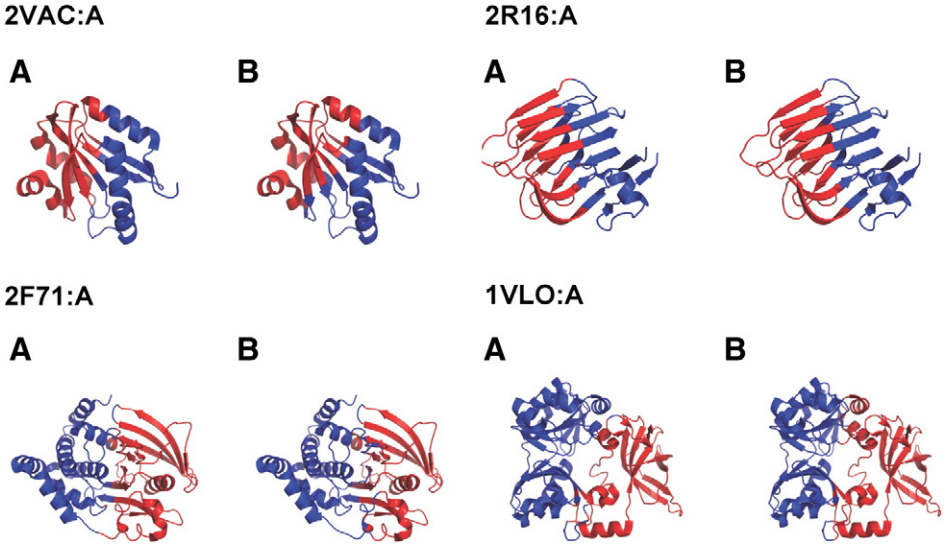

Fig. 2. Comparison of normal mode displacements along the slowest mode. The proteins examined in Fig. 1 are selected for demonstration. The corresponding diagrams are shown with our method on the left panel and the GNM on the right. The regions color-coded in red and blue indicate the opposite directions of the displacement of the modes.

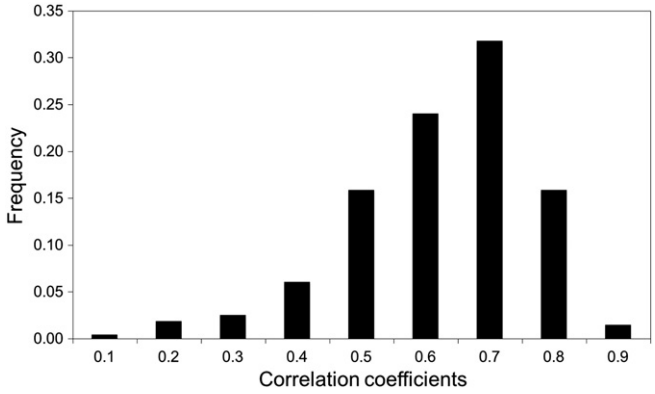

Fig. 3. Distribution of correlation coefficients between correlation maps produced by our method and the GNM. The distribution of correlation coefficients between correlation maps calculated based on our method and the GNM for the 100-dataset is shown.

isomerase) of the 100-dataset. Figs. 4D and E show performance distributions under monoclinic, orthorhombic, tetragonal, trigonal crystal lattices, and for various solvent contents, respectively. Figs. 4F and G present the method's performances as functions of the structure resolution and R-value. We excluded marginal fractions of less than five proteins. The average performances in the examined ranges are comparable for all characteristics, suggesting that atomic cross-correlations computed using our method are not influenced by the diverse properties of proteins.

3.4. The application of our method in protein functional studies

It is common to use normal mode motions for analyzing protein functional dynamics. Here, we illustrate the applicability of our method to protein functional studies using dihydrodipicolinate reductase (PDB ID: 1ARZ) and ketoacyl–acyl carrier protein synthase (PDB ID: 1B3N) structures.

3.5. Dihydrodipicolinate reductase

Dihydrodipicolinate reductase is to catalyze the NADH (or NADPH)-dependent reduction (Scapin et al., 1997). We modeled the entire 1ARZ chain D: 3-273 as a single TLS group, and optimized the parameters by running 15 cycles of TLS refinement, followed by 10 restrained refinement cycles. The resulting TLS parameters and the output coordinates were used to compute a correlation map. The corresponding normal mode vectors and frequencies were obtained through diagonalizing the 1ARZ:D dynamic correlations matrix. Analysis of the first three slow modes showed that the normal motion computed using our method was similar to that derived using the GNM (Fig. 5A, lower panel). A recent study (Yang and Bahar, 2005), reported that the catalytic residues (H159, H160, and K163) and the 1ARZ:D ligand-binding residues (R16, M17, R81, G102, T104, A127, F129, K163, G169 and T170) (Fig. 5A, upper panel) were immobilized because of their location at the crossover region between two opposite substructures. Similar correlated motions are apparent from our own analysis.

3.6. Ketoacyl–acyl carrier protein synthase 2

The major function of Ketoacyl–acyl carrier protein synthase is to catalyze chain elongation in fatty acid biosynthesis (Moche et al., 1999). The REFMAC program was applied to 1B3N chain A: 2-412. To determine the TLS parameters, 15 cycles of TLS refinement, followed by 10 restrained refinement cycles were performed, and output coordinates were used for computing the correlation map. The slowest three eigenvectors were calculated from diagonization of the resulting correlation map. The lower part of Fig. 5B shows the eigen motions computed using on our method and the GNM. The correlation between these two eigen motions is relatively high, with a correlation coefficient of 0.80. Additionally, the catalytic residues (C163, F398, G399 and F400) and the ligand-binding residues (G107, I108, C163, A193, G198, F202, H303, H340 and L342), presented in the upper panel of Fig. 5B, are also located at the crossover region, and undergo opposing correlated motions as the case illustrated in Fig. 5A. These results demonstrate the viability of our method for providing insight into the structure–dynamics–function relationship.

4. Discussion

In this study, we found that correlations between fluctuations of residues can be simply obtained from structure refinement data by using TLS parameters, without the need for complicated simulations. We conducted several comparisons between our method and commonly used GNM approach, and our findings indicated excellent agreement between the two methodologies.

Because the TLS parameters are directly refined against X-ray experimental data, the correlated motions derived from the TLS parameters reflect real situations that exist within the protein molecule. Although the rigid-body assumption of using TLS parameters to model protein motions sacrificed detailed information, the large-scale dynamics of the protein molecule are preserved. Hence, it is both practical and reasonable to extract correlated motions between residues from these TLS parameters. However, use of the rigid-body assumption only allows the lowest-frequency motions to be captured. Fortunately, many literature reports suggest that functional motions commonly correspond to the slowest modes (Amadei et al., 1993; Hinsen, 1998, 2000; Tama and Sanejouand, 2001; Thomas et al., 1999). As we described above, correlated motions derived using our method can successfully explain the mechanisms of various protein functions. However, it should be noted that Eq. (2) is an empirical relationship, determined from results and not by derivation. Hence, further investigation is required to understand equation's physical basis.

Additionally, Eq. (2) uses the assumption that all atoms to be calculated are in the same domain (i.e., the same TLS group), however, there are many proteins whose structures contain more than one domain. According to our statistics for non-redundant protein structures in SCOP 1.75 (Murzin et al., 1995), 20% of the proteins are multi-domain structures, compared to 80% for single-domain structures. Therefore, it is necessary to evaluate the effect of treating a multi-domain structure as a single TLS group. Because the domain information for most protein structures in our dataset is not defined in SCOP 1.75, we ran a Protein Domain Parser (Alexandrov and Shindyalov, 2003), which is a domain prediction program, to calculate number of protein domains for each structure in our dataset. The results show that 65% of the proteins in our dataset are single-domain structures while 35% are multi-domain structures. We treat each protein chain in our dataset as a single TLS group regardless of whether there were multiple domains in the protein chain. The resulting average correlation coefficients for multi-domain structures and single-domain structures are 0.76 and 0.74, respectively. The student's t-test did not show significant difference between these two distributions ($p > .05$). This suggests that treating multiple domains as a single TLS group may not significantly affect our model's atomic cross-correlation computations, and implies that the dynamic properties of a TLS group adequately describe those of a protein domain.

5. Conclusions

Atomic cross-correlations provide information of long-distance dynamic couplings and collective motions of protein chains, and help researchers to determine possible functional mechanisms. In this study, we describe a novel approach to obtain correlated motions directly from X-ray structure refinement data by using X-ray spectral

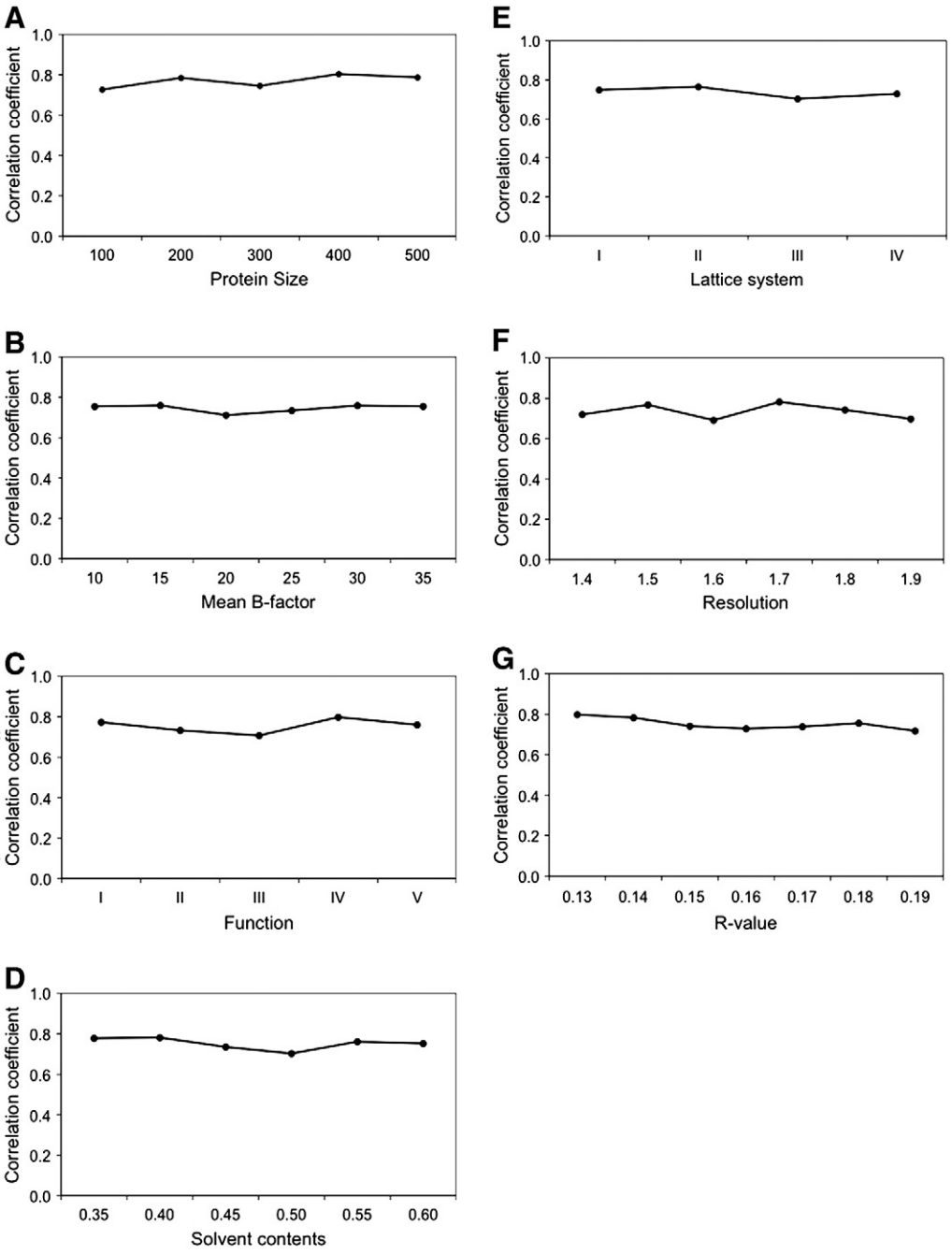

Fig. 4. Distributions of correlation coefficients between correlation maps as functions of various protein characteristics. The correlation coefficient between correlation maps based on the our method and the GNM for the 100-dataset as a function of (A) the protein size, (B) the overall mean B-value, (C) the top five functions in quantity (i.e., I: Hydrolase, II: Transferase, III: Oxidoreductase, IV: Lyase and VI: Isomerase), (D) the solvent contents, (E) the crystal lattices (i.e., I: Monoclinic, II: Orthorhombic, III: Tetragonal and IV: Trigonal), (F) the x-ray structure resolution, and (G) the R-value.

TLS parameters. Our results show that our approach is both practical and plausible, and has potential for application in protein functional studies. Because this method uses the same set of TLS parameters as those used in general TLS refinement process, it is straightforward for structure biologists to apply. In addition, because the correlation map can be obtained directly along with a refined protein structure, structure–dynamics–function relationships are easily constructed.

Supplementary data to this article can be found online at http://dx.doi.org/10.1016/j.gene.2012.11.086.

Competing interests

The authors report no conflict of interest.

Authors' contributions

Original idea: JKH. Design of this method: JKH, YYL, CHS. Evaluation perform: YYL and CHS. Data analysis and discussion: YYL and CCC. Manuscript preparation: YYL and CCC.

Acknowledgments

This research was supported in part by Academic Summit Program of the National Science Council with grant number 100-2745-B-009-001-ASP (JKH) and the Center of Bioinformatics Research of Aiming for the Top University Program (JKH) of the National Chiao Tung University and Ministry of Education, Taiwan, ROC.

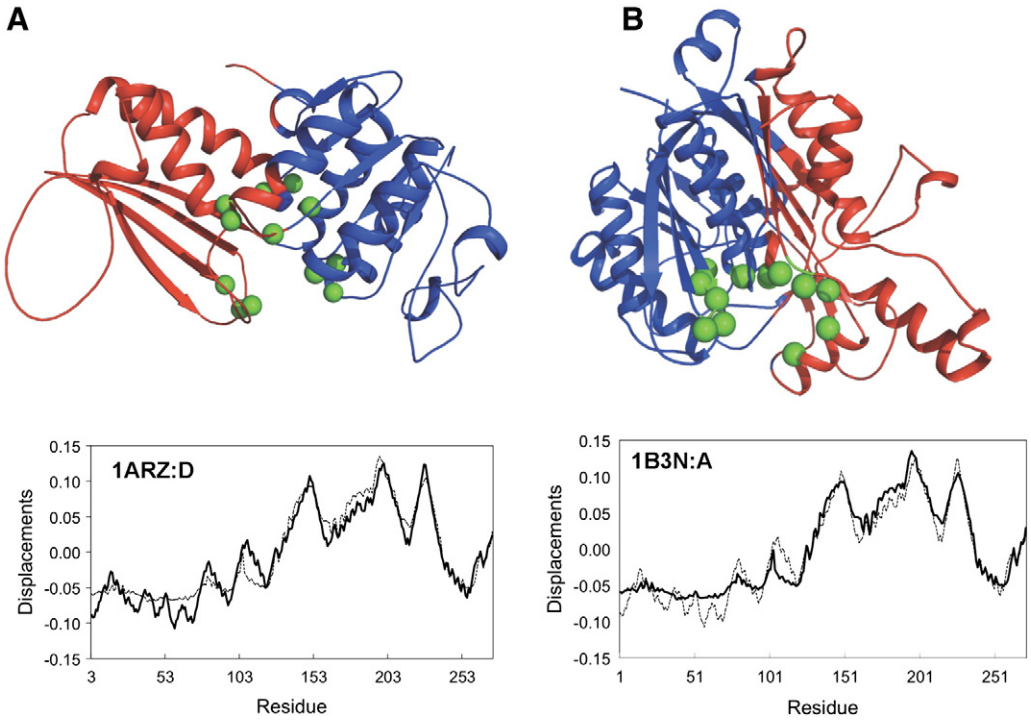

Fig. 5. The normal mode displacements of (A) dihydrodipicolinate reductase (1ARZ:A) and (B) ketoacyl–acyl carrier protein synthase (1B3N:A) are shown. The solid line presents the displacement calculated using our method, and the dash line is based on the GNM. The upper panels of (A) and (B) show the slow modes computed based on our method with the catalytic and binding residues shown in green spheres (only Cα atoms are shown). The regions colored in red and blue indicate the opposite directions of the displacement of the modes.

References

Alexandrov, N., Shindyalov, I., 2003. PDP: protein domain parser. Bioinformatics 19, 429–430.

Altman, R.B., Hughes, C., Jardetzky, O., 1994. Compositional characteristics of disordered regions in proteins. Protein Pept. Lett. 1, 120–128.

Amadei, A., Linssen, A.B.M., Berendsen, H.J.C., 1993. Essential dynamics of proteins. Proteins Struct. Funct. Genet. 17, 412–425.

Ansari, A., et al., 1986. Ligand binding to heme proteins: relevance of low-temperature data. Biochemistry 25, 3139–3146.

Austin, R.H., Beeson, K.W., Eisenstein, L., Frauenfelder, H., Gunsalus, I.C., 1975. Dynamics of ligand binding to myoglobin. Biochemistry 14, 5355–5373.

Bahar, I., Atilgan, A.R., Erman, B., 1997. Direct evaluation of thermal fluctuations in proteins using a single-parameter harmonic potential. Fold. Des. 2, 173–181.

Brooks, B., Karplus, M., 1983. Harmonic dynamics of proteins: normal modes and fluctuations in bovine pancreatic trypsin inhibitor. Proc. Natl. Acad. Sci. U. S. A. 80, 6571–6575.

Brooks, B.R., Bruccoleri, R.E., Olafson, B.D., States, D.J., Swaminathan, S., Karplus, M., 1983. CHARMM — a program for macromolecular energy, minimization, and dynamics calculations. J. Comput. Chem. 4, 187–217.

Brooks III, C.L., Karplus, M., Pettitt, B.M., 1988. Advances in Chemical Physics, Proteins: A Theoretical Perspective of Dynamics, Structure, and Thermodynamics. John Wiley and Sons, New York.

Carugo, O., Argos, P., 1998. Accessibility to internal cavities and ligand binding sites monitored by protein crystallographic thermal factors. Proteins 31, 201–213.

Case, D.A., Karplus, M., 1979. Dynamics of ligand binding to heme proteins. J. Mol. Biol. 132, 343–368.

Cruickshank, D., 1956. The analysis of the anisotropic thermal motion of molecules in crystals. Acta Crystallogr. 9, 754–756.

Driessen, H., Haneef, M.I.J., Harris, G.W., Howlin, B., 1989. RESTRAIN — restrained structure-factor least-squares refinement program for macromolecular structures. J. Appl. Crystallogr. 22, 510–516.

Elber, R., Karplus, M., 1987. Multiple conformational states of proteins: a molecular dynamics analysis of myoglobin. Science 235, 318–321.

He, X.M., Craven, B.M., 1993. Internal vibrations of a molecule consisting of rigid segments. I. Non-interacting internal vibrations. Acta Crystallogr. A 49 (Pt 1), 10–22.

Hinsen, K., 1998. Analysis of domain motions by approximate normal mode calculations. Proteins Struct. Funct. Genet. 33, 417–429.

Hinsen, K., 2000. Domain motions in proteins. J. Mol. Liq. 84, 53–63.

Howlin, B., Butler, S.A., Moss, D.S., Harris, G.W., Driessen, H.P.C., 1993. TLSANL — TLS parameter-analysis program for segmented anisotropic refinement of macromolecular structures. J. Appl. Crystallogr. 26, 622–624.

Jorgensen, W.L., Tirado-Rives, J., 1988. The OPLS [optimized potentials for liquid simulations] potential functions for proteins, energy minimizations for crystals of cyclic peptides and crambin. J. Am. Chem. Soc. 110, 1657–1666.

Karplus, M., Post, C.B., 1996. Simulations of lysozyme: internal motions and the reaction mechanism. EXS 75, 111–141.

Kidera, A., Go, N., 1992. Normal mode refinement: crystallographic refinement of protein dynamic structure. I. Theory and test by simulated diffraction data. J. Mol. Biol. 225, 457–475.

Kubitzki, M.B., Groot, B.L.d, Seeliger, D., 2009. Protein dynamics: from structure to function. In: Rigden, D.J., Rigden, D.J. (Eds.), From Protein Structure to Function with Bioinformatics. Springer, pp. 217–249.

Kuriyan, J., Weis, W.I., 1991. Rigid protein motion as a model for crystallographic temperature factors. Proc. Natl. Acad. Sci. U. S. A. 88, 2773–2777.

Levitt, M., Warshel, A., 1975. Computer simulation of protein folding. Nature 253, 694–698.

Levitt, M., Sander, C., Stern, P.S., 1985. Protein normal-mode dynamics: trypsin inhibitor, crambin, ribonuclease and lysozyme. J. Mol. Biol. 181, 423–447.

McCammon, J.A., Harvey, S.C., 1986. Dynamics of Proteins and Nucleic Acids. Cambridge University Press, Cambridge.

McCammon, J.A., Gelin, B.R., Karplus, M., 1977. Dynamics of folded proteins. Nature 267, 585–590.

Ming, D., Kong, Y.F., Lambert, M.A., Huang, Z., Ma, J.P., 2002. How to describe protein motion without amino acid sequence and atomic coordinates. Proc. Natl. Acad. Sci. U. S. A. 99, 8620–8625.

Moche, M., Schneider, G., Edwards, P., Dehesh, K., Lindqvist, Y., 1999. Structure of the complex between the antibiotic cerulenin and its target, beta-ketoacyl–acyl carrier protein synthase. J. Biol. Chem. 274, 6031–6034.

Murshudov, G.N., Vagin, A.A., Dodson, E.J., 1997. Refinement of macromolecular structures by the maximum-likelihood method. Acta Crystallogr. D Biol. Crystallogr. 53, 240–255.

Murzin, A.G., Brenner, S.E., Hubbard, T., Chothia, C., 1995. SCOP — a structural classification of proteins database for the investigation of sequences and structures. J. Mol. Biol. 247, 536–540.

Parak, F., Knapp, E.W., 1984. A consistent picture of protein dynamics. Proc. Natl. Acad. Sci. U. S. A. 81, 7088–7092.

Parthasarathy, S., Murthy, M.R.N., 2000. Protein thermal stability: insights from atomic displacement parameters (B values). Protein Eng. 13, 9–13.

Ponder, J.W., Case, D.A., 2003. Force fields for protein simulations. Protein Simul. 66 (27-+).

Post, C.B., et al., 1986. Molecular dynamics simulations of native and substrate-bound lysozyme. A study of the average structures and atomic fluctuations. J. Mol. Biol. 190, 455–479.

Radivojac, P., et al., 2004. Protein flexibility and intrinsic disorder. Protein Sci. 13, 71–80.

Rasmussen, B.F., Stock, A.M., Ringe, D., Petsko, G.A., 1992. Crystalline ribonuclease A loses function below the dynamical transition at 220 K. Nature 357, 2.

Rueda, M., et al., 2007. A consensus view of protein dynamics. Proc. Natl. Acad. Sci. U. S. A. 104, 796–801.

Scapin, G., Reddy, S.G., Zheng, R., Blanchard, J.S., 1997. Three-dimensional structure of *Escherichia coli* dihydrodipicolinate reductase in complex with NADH and the inhibitor 2,6-pyridinedicarboxylate. Biochemistry 36, 15081–15088.

Schomaker, V., Trueblood, K.N., 1968. On the rigid-body motion of molecules in crystals. Acta Crystallogr. B 24, 63–76.

Schushan, M., Barkan, Y., Haliloglu, T., Ben-Tal, N., 2010. C alpha-trace model of the transmembrane domain of human copper transporter 1, motion and functional implications. Proc. Natl. Acad. Sci. U. S. A. 107, 10908–10913.

Scott, W.R.P., et al., 1999. The GROMOS biomolecular simulation program package. J. Phys. Chem. A 103, 3596–3607.

Solá, R.J., Griebenow, K., 2006. Influence of modulated structural dynamics on the kinetics of α-chymotrypsin catalysis. FEBS J. 273, 5303–5319.

Sternberg, M.J., Grace, D.E., Phillips, D.C., 1979. Dynamic information from protein crystallography. An analysis of temperature factors from refinement of the hen egg-white lysozyme structure. J. Mol. Biol. 130, 231–252.

Strynadka, N.C., James, M.N., 1996. Lysozyme: a model enzyme in protein crystallography. EXS 75, 185–222.

Szarecka, A., Xu, Y., Tang, P., 2007a. Dynamics of heteropentameric nicotinic acetylcholine receptor: implications of the gating mechanism. Proteins Struct. Funct. Genet. 68, 948–960.

Szarecka, A., Xu, Y., Tang, P., 2007b. Dynamics of firefly luciferase inhibition by general anesthetics: Gaussian and anisotropic network analyses. Biophys. J. 93.

Tama, F., Sanejouand, Y.H., 2001. Conformational change of proteins arising from normal mode calculations. Protein Eng. 14, 1–6.

Thomas, A., Hinsen, K., Field, M.J., Perahia, D., 1999. Tertiary and quaternary conformational changes in aspartate transcarbamylase: a normal mode study. Proteins Struct. Funct. Genet. 34, 96–112.

Tirion, M.M., 1996. Large amplitude elastic motions in proteins from a single-parameter, atomic analysis. Phys. Rev. Lett. 77, 1905–1908.

Toncrova, H., McLeish, T.C.B., 2010. Substrate-modulated thermal fluctuations affect long-range allosteric signaling in protein homodimers: exemplified in CAP. Biophys. J. 98, 2317–2326.

Valadie, H., Lacapcre, J.J., Sanejouand, Y.H., Etchebest, C., 2003. Dynamical properties of the MscL of *Escherichia coli*: a normal mode analysis. J. Mol. Biol. 332, 657–674.

Wang, G., Roland, L., Dunbrack, J., 2003. PISCES: a protein sequence culling server. Bioinformatics 19, 1589–1591.

Warshel, A., 1976. Bicycle-pedal model for the first step in the vision process. Nature 260, 679–683.

Warshel, A., 2002. Molecular dynamics simulations of biological reactions. Acc. Chem. Res. 35, 385–395.

Winn, M.D., Isupov, M.N., Murshudov, G.N., 2001. Use of TLS parameters to model anisotropic displacements in macromolecular refinement. Acta Crystallogr. D Biol. Crystallogr. 57, 122–133.

Yang, L.W., Bahar, I., 2005. Coupling between catalytic site and collective dynamics: a requirement for mechanochemical activity of enzymes. Structure 13, 893–904.

Yuan, Z., Zhao, J., Wang, Z.X., 2003. Flexibility analysis of enzyme active sites by crystallographic temperature factors. Protein Eng. 16, 109–114.